ChemPubSoc Europe

DOI: 10.1002/chem.201902681

A European Journal Full Paper

Small Ring Systems | *Hot Paper*

Reactivity of a Sterically Unencumbered α-Borylated Phosphorus Ylide towards Small Molecules

Michael Radius, Ewald Sattler, Helga Berberich, and Frank Breher*[a]

Abstract: The influence of substituents on α-borylated phosphorus ylides (α-BCPs) has been investigated in a combined experimental and quantum chemical approach. The synthesis and characterization of $Me_3PC(H)B(iBu)_2$ (**1**), consisting of small Me substituents on phosphorous and *i*Bu residues on boron, is reported. Compound **1** is accessible through a novel synthetic approach, which has been further elucidated through DFT studies. The reactivity of **1** towards various small molecules was probed and compared with that of a previously published derivative, $Ph_3PC(Me)BEt_2$ (**2**). Both α-BCPs react with NH_3 to undergo heterolytic N–H bond cleavage. Different di- and trimeric ring structures were observed in the reaction products of **1** with CO and CO_2. With PhNCO and PHNCS, the expected insertion products $[Me_3PC(H)(PhNCO)B(iBu)_2]$ and $[Me_3PC(H)(PhNCS)B(iBu)_2]$, respectively, were isolated.

Introduction

Since the discovery of the activation of dihydrogen by a compound containing a main-group element by Power et al. in 2005,[1] and the reversible cleavage of dihydrogen reported by Stephan et al. in 2006,[2] the field of molecules based on main-group elements, mimicking transition-metal chemistry—for example, small-molecule activation—has quickly developed.[3] The most prominent group of compounds are the frustrated Lewis pairs (FLPs), in which a Lewis acid and a Lewis base are hindered during inter- or intramolecular combination.[4] However, FLP-type reactivity is not only observed for unquenched Lewis pairs. For instance, carbenes, which inherently feature ambiphilic character, are also able to react with, for example, H_2 or NH_3.[5] Heteroalkenes possessing perturbed element–element double bonds also show FLP-type reactivity towards small molecules.[6] In 2008, Stephan et al. reported on the addition of H_2 to a phosphinoborane (Scheme 1).[6h] Recently, it has been demonstrated that conjugated, boron-substituted multiple bonds show ambiphilic reactivity.[7] Accordingly, Stephan and Erker noted that "borate alkenes can be viewed as FLPs with adjacent donor and acceptor sites".[4e,8] Our group recently reported on an α-borylated phosphorus ylide (α-BCP),[9] featuring a highly polarized borataalkene subunit.[10a] We found that the α-BCP readily reacted with CO, CO_2, COS, CS_2, PhNCO, and PhNCS (Scheme 1).[10a]

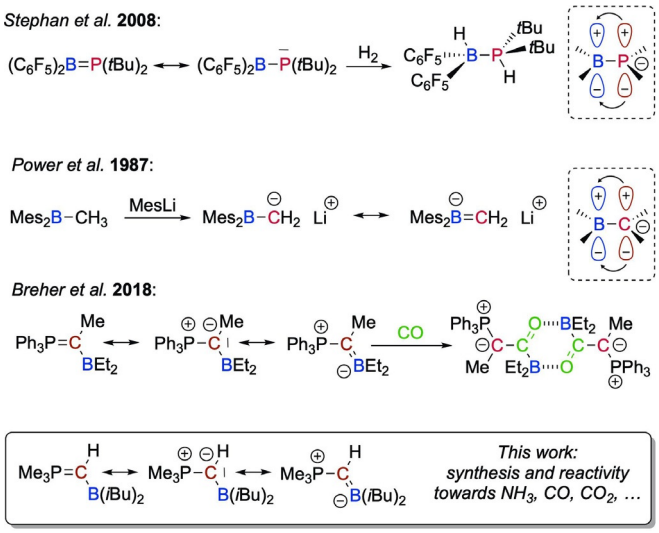

Scheme 1. Structures and reactivity of selected heteroalkenes. Mes = mesityl.

To probe whether the reactivity of α-BCPs could be modified by changing the substituent pattern, we became interested in studying α-BCPs with small Me substituents on the phosphorus atom.

Results and Discussion

We first targeted the smallest possible α-BCP, that is, the all-Me-substituted derivative, $Me_3PC(H)BMe_2$. However, transylidation[11] of $Me_3PC(H)_2B(Br)Me_2$ with Me_3PCH_2 did not lead to the desired target structure, at least in our hands. The main product of the reaction was found to be the eight-membered ring

[a] M. Radius, Dr. E. Sattler, H. Berberich, Prof. Dr. F. Breher
Institute of Inorganic Chemistry, Division Molecular Chemistry
Karlsruhe Institute of Technology (KIT)
Engesserstr. 15, 76131 Karlsruhe (Germany)
E-mail: breher@kit.edu

Supporting information and the ORCID identification number(s) for the author(s) of this article can be found under: https://doi.org/10.1002/chem.201902681.

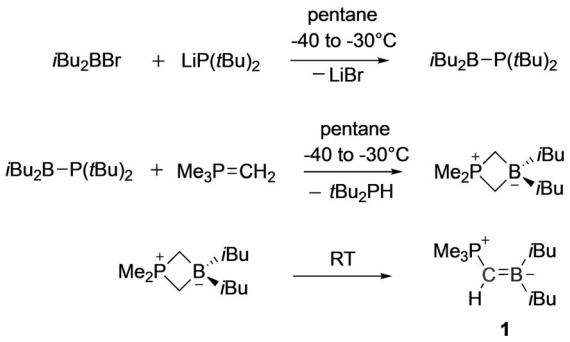

Scheme 2. Synthesis of **1**.

$[H_2C–PMe_2–CH_2–BMe_2]_2$. During our studies on phosphorous ylides, we found, by chance, that the reaction of $iBu_2B–P(tBu)_2$ with Me_3PCH_2 yielded $Me_3PC(H)B(iBu)_2$ (**1**; Scheme 2). The starting material $iBu_2B–P(tBu)_2$ was generated in situ to prevent isobutene elimination. The expected intermediate was isolated and we successfully obtained NMR spectroscopic evidence for the four-membered PC_2B ring structure, which is known from the literature.[12] The NMR spectroscopy measurement was conducted in $[D_8]$toluene at $-60\,^{\circ}C$. The $^{31}P\{^1H\}$ resonance is detected at $\delta = 27.6$ ppm, which is shifted about 25 ppm downfield relative to that of **1**. The ^{11}B NMR resonance, with a chemical shift of $\delta = -10.9$ ppm, is shifted about 60 ppm upfield relative to that of **1**. Overall, the chemical shifts fit perfectly to the inner salt character of the four-membered ring structure. The ^1H NMR resonances are detected at $\delta = 0.60$ ppm ($^2J(P,H) = 13.1$ Hz, 6H) for the hydrogen atoms of the P-bound methyl groups and at $\delta = 0.43$ ppm ($^2J(P,H) = 14.6$ Hz, 4H) for the bridging CH_2 groups. The couplings collapse if the ^1H NMR spectrum is recorded with ^{31}P decoupling. We note that the ^1H NMR resonances of the *i*Bu substituents are not perfectly isochronal, probably due to possible *endo*/*exo* positions (cf. the structure obtained through quantum chemical calculation).

Because ylides are very strong σ donors,[13] an initial coordination to the Lewis acidic boron atom of $iBu_2B–P(tBu)_2$ is very likely. To shed some light on the reaction mechanisms for the formation of **1**, we calculated the reaction pathway of the deprotonation of $Me_3P{=}CH_2$ and the formation of a four-membered ring (Figure 1). The Gibbs free energy for coordination of the ylide to the boron atom and formation of **P1** is slightly exergonic (-4 kJ mol^{-1}; Figure 1). The energy barrier to the six-membered ring that comprises the transition state for the proton shift from the methyl group to the phosphorus atom (product **P2**) was found to be only 27.9 kJ mol^{-1}, and thus, quite low. The subsequent dissociation of tBu_2PH is nearly without an energy barrier. The formation of the PC_2B four-membered ring compound **P3** and open α-BCP structure **P4** (i.e., **1**) are both highly exergonic (-119.8 and -136.6 kJ mol^{-1}, respectively). Rearrangement to α-BCP **1** can proceed either inter- or intramolecularly. Overall, these calculated Gibbs free energies are in good agreement with the reaction conditions.

Further quantum chemical calculations revealed a very similar electron distribution for **1** to that of a previously reported derivative, $Ph_3PC(Me)BEt_2$ (**2**).[10a] The calculated frontier orbitals are depicted in Figure 2, showing that the HOMO is mainly

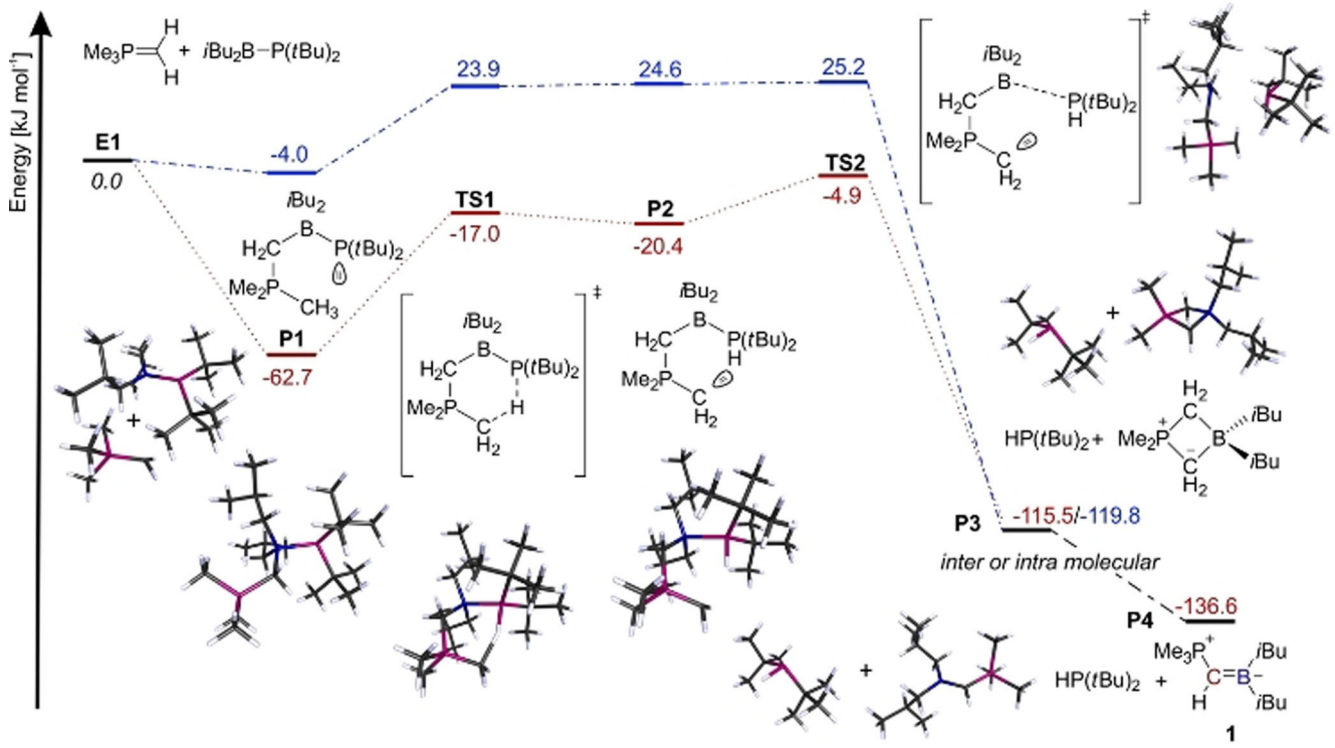

Figure 1. Calculated (BP86/(ri-)def2-SVP) reaction pathway, electronic energies (in red), and Gibbs free energies (in blue) to **1**. The free energies were calculated at 233.15 K.

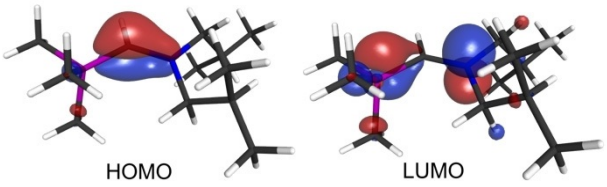

Figure 2. The calculated Kohn–Sham HOMO and LUMO of **1** (BP86/def2-TZVPP; isosurface value of 0.06).

comprised of the p-type C-based lone pair of electrons with a smaller coefficient on the boron atom. The LUMO is mainly comprised of the vacant p orbital on boron with part of the antibonding P–C_{Me} orbitals.

As for **2**, we calculated the fluoride ion affinity (FIA)[14] of **1** (BP86/def2-SVP). The FIA of **1** was found to amount to 196 kJ mol^{-1}, that is, about 30 kJ mol^{-1} lower than that of **2** (224 kJ mol^{-1}). The main difference in the electronic structure is caused by substitution of the C_{ylide}–hydrogen in **1** by the CH_3 group in **2**. This becomes clear if the natural population analysis charges are compared. To this end, we calculated charges for the model compounds **q1^{H}** and **q2^{Me}** and the hypothetical molecules **q1^{Me}** and **q2^{H}** with Me and H substituents on the ylidic carbon atoms, respectively (Scheme 3).

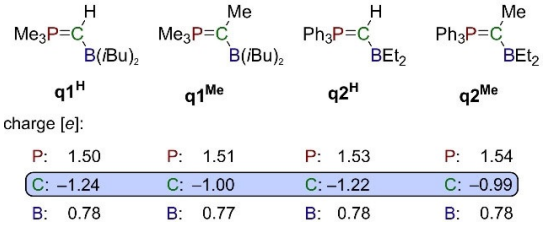

Scheme 3. Natural population analysis charges (BP86/def2-SVP) of **q1^{H}**, **q1^{Me}**, **q2^{H}**, and **q2^{Me}**.

Although the charges on the boron and phosphorus atoms do not change significantly, the charges on the ylidic carbon atoms for model compounds with a C_{ylide}–H bond (**q1^{H}**, **q2^{H}**) are more negative (−0.25 e) than that for the two methylated analogous **q1^{Me}** and **q2^{Me}**. It appears that this higher charge density is partly responsible for the lower FIA calculated for **1** and originates from the inability of the H substituent to participate in negative hyperconjugation. Nevertheless, the higher charge is not reflected in the Wiberg bond indices (WBI). The WBIs of the P–C_{ylide} and C_{ylide}–B bonds in **1** are calculated to be 1.28 and 1.41, respectively, and are thus very similar to those of **2** (P–C_{ylide}: 1.25, C_{ylide}–B: 1.42).[10a]

To further elucidate the influence of the other B- and P-bound substituents, we calculated the FIAs for several additional model compounds (**qR^{1}R^2**, with R^1 bound to the phosphorus atom and R^2 bound to the boron atom; R^1/R^2 = Me, Et, *i*Pr, Ph; Table 1). From this study, it becomes clear that, for small alkyl substituents, such as Me on boron, the FIA is clearly reduced (hyperconjugative effects). A further increase in the degree of alkylation upon going from **qMeMe** to **qMeEt** to **qMePr** gradually increases the FIA from 165 to 197 and 221 kJ mol^{-1}, respectively. Aryl groups, such as Ph, further increase the FIA to 231 kJ mol^{-1} (cf., Table 1, entry 4). The highest FIA was found for the all-Ph derivative, **qPhPh** (Table 1, entry 8; 266 kJ mol^{-1}). Also, the influence of substituents on the phosphorus atom is significant. This may be due to the higher Lewis acidity of the PR$^1_3$ fragment because of lowering of the σ*(P–C) orbitals. These trends correlate well with the electronegativity (increasing from Me to Et, *i*Pr, and Ph) of the substituents.[15] Interestingly, the calculated C–B bond lengths remain almost the same for the whole series of model compounds.

Table 1. Calculated (BP86/def2-SVP) FIA and C–B bond lengths for different model compounds.

Entry	Compound	FIA [kJ mol^{-1}]	*d*(C–B) [pm]
1	$Me_3PC(Me)BMe_2$ (**qMeMe**)	165	151.0
2	$Me_3PC(Me)BEt_2$ (**qMeEt**)	197	150.8
3	$Me_3PC(Me)B(iPr)_2$ (**qMePr**)	221	151.5
4	$Me_3PC(Me)BPh_2$ (**qMePh**)	231	150.3
5	$Et_3PC(Me)BMe_2$ (**qEtMe**)	181	151.1
6	$iPr_3PC(Me)BMe_2$ (**qPrMe**)	196	151.4
7	$Ph_3PC(Me)BMe_2$ (**qPhMe**)	226	151.6
8	$Ph_3PC(Me)BPh_2$ (**qPhPh**)	266	150.8

To probe the reactivity of **1**, we performed reactions with various small molecules. As with **2**,[10a] compound **1** does not react with dihydrogen, but the reaction with NH_3, which possesses a relatively strong N–H bond (D = 446 kJ mol^{-1}),[16] smoothly proceeds at room temperature with both ylides **1** and **2**. The corresponding ylide and the aminoborane R_2B–NH_2 are formed (Scheme 4), as evidenced by ^{11}B and ^{31}P NMR spectroscopic investigations. The $^{31}P\{^1H\}$ NMR chemical shifts clearly indicate the formation of the ylides. The ^{11}B NMR resonances are shifted upfield from δ = 56.5 to 48.7 ppm for **2** and from δ = 54.7 ppm to 47.6 ppm for **1**, respectively; these values perfectly match those reported in the literature for R_2B–NH_2.[17]

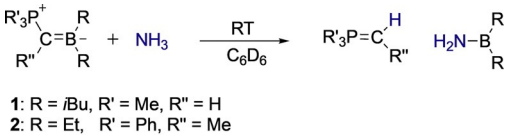

Scheme 4. Reaction of **1** and **2** with NH_3 at room temperature.

It should be noted that precedents for such reactivity have been published previously for dialkyl boron compounds. The splitting of NH_3 with the formation of R_2B–NH_2 takes place in boron compounds featuring Lewis basic substituents, such as R_2B–SEt, or with *t*BuC(O)O–BEt_2.[18]

Compound **1** reacts at elevated temperatures with CO in toluene. However, the structure of the product (**3**) differs from that found for **2**. Whereas the latter forms a dimeric structure (Scheme 5), compound **1** forms an adduct with another equivalent of α-BCP.

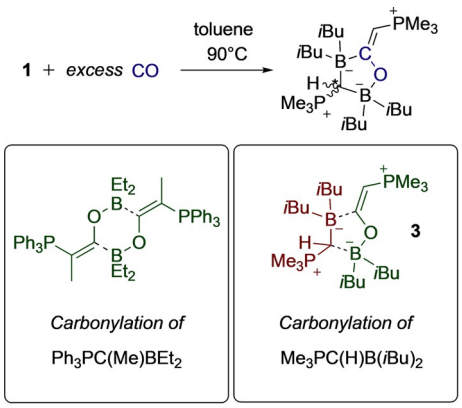

Scheme 5. Reaction of **1** with CO to form **3** and a comparison with the reactivity found for **2**.[10a]

Single crystals of **3** suitable for XRD studies were obtained from a solution in hexane at room temperature (Figure 3). The space group for **3** is $P2_1/c$ and, since **3** comprises a stereocenter at C2, both enantiomers are present in the solid state. The core structure is composed of a five-membered C_2OB_2 heterocycle with C2 residing about 15° above the plane spanned by the atoms B2, C3, O1, and B1. The P1–C1 bond length of 1.723 Å falls in the typical range for stabilized ylidic bonds.[10a] The analogous P2–C2 bond (1.742 Å) is slightly elongated. As expected, the distances C1–C3 (1.398 Å) and C3–O1 (1.334 Å) fall between that of typical single- and double-bond lengths. The carbon–boron bond lengths are in the expected range.

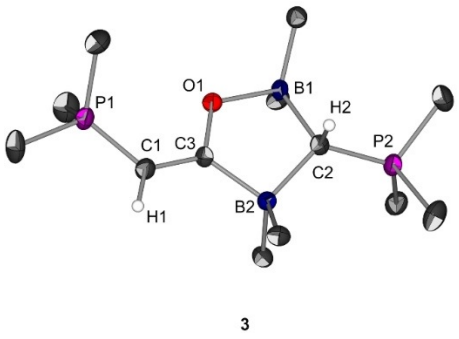

Figure 3. ORTEP view (ellipsoids at the 30% probability level) of **3**. Hydrogen atoms (except H1 and H2) and the C(H)Me_2 part of the *i*Bu groups are omitted for clarity. Only the main part of the disordered structure is depicted. Selected bond lengths [Å] and angles [°]: P1–C1 1.723(4), P2–C2 1.742(3), C1–C3 1.398(8), C3–O1 1.334(8), C3–B2 1.627(7), C2–B2 1.689(5), C2–B1 1.672(5), B1–O1 1.557(5); C3-C1-P1 121.6(4), O1-C3-C1 114.3(5), C1-C3-B2 129.6(7), B1-C2-B2 105.7(3).

The ylidic carbon atom C1 adopts a trigonal planar coordination environment in the crystal structure. However, as reported by Mitzel et al.,[19] the solid-state structure is not always representative of the local geometry of an ylidic carbon atom in solution or in the gas phase. Indeed, we detected in solution two well-separated chemical shifts for H1 and P2 in the ^{1}H and ^{31}P NMR spectrum, respectively, both integrating with values of 1:1 (Figure 4). This can most likely be attributed to the presence of two diastereomers, that is, a second stereocenter in addition to that at C2 depicted in Figure 4. This suggests that the local geometry of the ylidic carbon atom is not planar, but (slightly) pyramidal;[20] thus providing a second stereocenter at C1. Interchange of one diastereomer into another through pyramidal inversion at C1 leads naturally to the uniformly distributed intensities (1:1).[21]

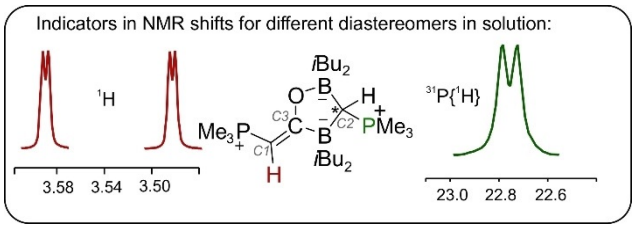

Figure 4. Sections of the ^{1}H and ^{31}P{^{1}H} NMR spectra of **3**. Atom numbering in the schematic drawing according to that given in Figure 3.

The different reactivity of **1** towards CO compared with that of **2** may, at least in part, be explained by the lower FIA of **1**. Quantum chemical calculations predicted the insertion/ylide adduct **3** to be 38 kJ mol^{-1} more stable than the hypothetical dimeric insertion product found for **2**.

The reactivity of **1** towards CO_2 has also been investigated. Again, the product (**4**) differs considerably from the product observed for **2** with CO_2 (Scheme 6). Interestingly, the reaction

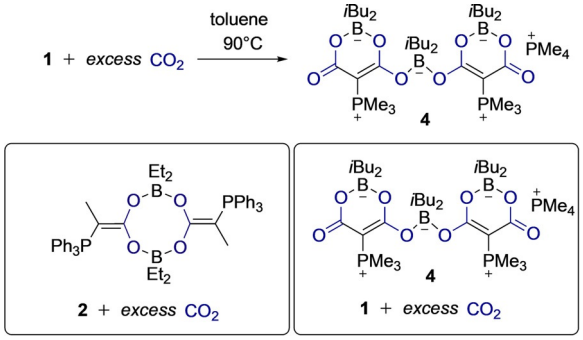

Scheme 6. Reaction of **1** with CO_2 to form **4** and a comparison with the reactivity found for **2**.

product is formed by three α-BCPs and four CO_2 molecules. Two molecules of **1** directly react with CO_2, each of which with two molecules of CO_2. Six-membered ring structures of the insertion products are formed, both of which are deprotonated by the third molecule of **1** to form $[PMe_4]^+$ and a $\{B(iBu)_2\}^+$ fragment. The latter is attached to the newly formed six-membered rings to give an overall negatively charged borate. Thus, as in the reaction product of **2** with CO_2, the boron atoms are saturated by binding to two oxygen atoms. In the reaction of **2** with CO_2, however, the methyl group inhibits further reaction similar to that displayed by **1**.

Single crystals of **4** suitable for XRD studies were obtained from toluene at room temperature (space group $P\bar{1}$; Figure 5). The structural parameters of only one half of the anion are discussed because the second half is metrically similar. The Me_4P^+

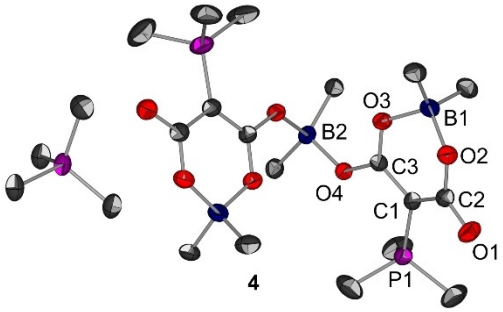

Figure 5. ORTEP view (ellipsoids at the 30% probability level) of **4**. Hydrogen atoms and the C(H)Me_2 part of the *i*Bu groups are omitted for clarity. Only the main part of the disordered structure is depicted. Selected bond lengths [Å] and angles [°] (the structural parameters of only one half of the anion are given because the second half is metrically similar): P1–C1 1.747(2), C1–C2 1.438(2), C1–C3 1.414(2), C2–O1 1.237(2), C2–O2 1.322(2), C3–O3 1.282(2), C3–O4 1.292(2), B1–O2 1.517(2), B1–O3 1.555(2), B2–O4 1.543(2); C2-C1-C3 119.8(2).

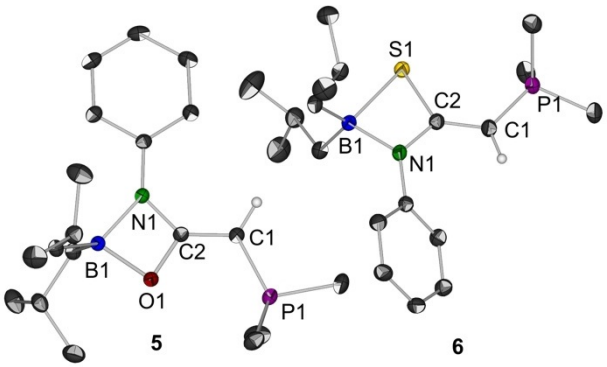

Figure 6. ORTEP views (ellipsoids at the 30% probability level) of **5** and **6**. Hydrogen atoms (except the ylidic hydrogen atom) are omitted for clarity. Selected bond lengths [Å] and angles [°]: **5**: P1–C1 1.723(2), C1–C2 1.376(2), N1–C2 1.353(2), O1–C2 1.331(2), N1–B1 1.603(2), O1–B1 1.593(2); P1-C1-C2 119.2(1), N1-C2-O1 101.3(1), C2-N1-B1 88.0(1), C2-O1-B1 89.2(1), N1-B1-O1 81.0(1). **6**: P1–C1 1.720(2), C1–C2 1.378(3), N1–C2 1.349(2), S1–C2 1.752(2), N1–B1 1.585(3), S1–B1 2.082(2); P1-C1-C2 124.58(15), N1-C2-S1 102.5(1), C2-N1-B1 102.6(1), C2-S1-B1 72.92(8), N1-B1-S1 81.9(1).

cation shows expected structural parameters.[22] Although the C1–C2 bond length of 1.438 Å is slightly longer than the corresponding C1–C3 bond of 1.414 Å, both still adopt values between those of C–C single and double bonds. The carbon–oxygen distances range from 1.237 Å for C2–O1 to 1.322 Å for C2–O2. The P1–C1 bond length (1.747 Å) indicates a small ylidic contribution. All B–O distances are in the expected range.[23]

The NMR spectroscopic characterization fully supported the structure of **4** found in the solid state. For instance, two well-separated ^{13}C NMR chemical shifts are found for the C$\underline{C}O_2$ entities at $\delta = 174.0$ and 171.8 ppm. In the ^{11}B NMR spectrum, only one broad resonance is detected at $\delta = -14.9$ ppm. Although the bridging boron moiety (B2) and the boron moieties in the six-membered rings possess slightly distinct environments, the differences are probably not significant enough to cause two distinct ^{11}B NMR shifts.

The α-BCP **1** also reacts with PhNCO and PhNCS. The reaction products are analogous to those observed for **2**. In each case, one PhNCX molecule inserts into the C_{ylidic}–B bond of one α-BCP and the boron atom is chelated by the nitrogen and chalcogen atoms (Scheme 7).[10a]

Scheme 7. Reaction of **1** with PhNCO and PhNCS to form **5** and **6**.

We note that the reaction products **5** and **6** thermally decompose easily. In the case of **5**, above about 60 °C and in the case of **6** at a slightly higher temperature of 89 °C. This may be due to greater ring strain in the small NBOC four-membered ring of **5** compared with the widened NBSC ring of **6**.

Single crystals of **5** (space group $P2_1/n$) and **6** (space group $P\bar{1}$) suitable for XRD studies were obtained from solutions in benzene toluene/pentane, respectively. The molecular structures are depicted in Figure 6 and the bond lengths and angles are very similar to published values. An interesting structural feature of **6** is the exceptionally long B1–S1 bond length of 2.082 Å, which indicates the formation of a weak B1···S1 contact instead of a strong bond. The corresponding bond length B1–O1 in **5** (1.593 Å) is slightly elongated relative to the boron–oxygen bonds in **3** and **4** (1.52–1.56 Å). These structural features, together with the low decomposition temperature, clearly support the view of strained four-membered rings. The NMR spectra of **5** and **6** are very similar (see the Experimental Section).

Conclusions

The fundamental reactivity of an α-BCP was untouched by substitution of the P-bound phenyl groups with methyl groups and reactions occurred with NH_3, CO, CO_2, PhNCO, and PhNCS. However, in the case of CO and CO_2, different products and structures were observed for **1** to those of previously published derivative **2**. In part, the different reaction patterns can be explained by different FIAs of both α-BCPs. Nevertheless, the presence of a C_{ylide}–H bond in **1** is also responsible for secondary reactions that arise from this reactive functional group.

Experimental Section

General

All operations were conducted under a dry argon atmosphere by using standard Schlenk and glovebox techniques. Solvents were dried rigorously and degassed before use. $Me_3P{=}CH_2$,[24] iBu_2BCl,[25] and $LiP(tBu)_2$[26] were synthesized according to procedures reported in the literature. The chemical shifts are expressed in ppm and ^1H and ^{13}C signals are given relative to tetramethylsilane (TMS). Coupling constants (*J*) are given in Hertz as positive values, regardless of their real individual signs. The multiplicity of the signals is indi-

cated as s, d, q, sept, or m for singlet, doublet, quartet, septet, or multiplet, respectively. The assignments were confirmed, as necessary, with the use of 2D NMR correlation experiments. MS measurements were performed on an Advion expression^{L} CMS mass spectrometer under atomic pressure chemical ionization (APCI). IR spectra were measured with a Bruker Alpha spectrometer by using the attenuated total reflection (ATR) technique on powdered samples, and the data are quoted in wavenumbers (cm^{-1}). The intensity of the absorption band is indicated as vw (very weak), w (weak), m (medium), s (strong), vs (very strong), and br (broad). Melting points were measured with a Thermo Fischer melting point apparatus and are not corrected. Elemental analyses were carried out in the institutional technical laboratories of the Karlsruhe Institute of Technology (KIT).

Synthesis of 1

A suspension of LiP(tBu)$_2$ (7.61 g, 50.0 mmol) in pentane (200 mL) at −50 °C was slowly added to a solution of iBu$_2$BCl (7.67 g, 47.8 mmol) in pentane (200 mL). After stirring the suspension at −40 °C for 48 h, the suspension was filtered in the cold and washed with cold pentane. The residue was extracted with cold toluene. At −50 °C, a solution of $Me_3P{=}CH_2$ (1.85 g, 20.5 mmol) in pentane (50 mL) was added to form a white precipitate. After cold filtration, the precipitate was washed with cold pentane. (From this precipitate, the NMR spectrum of $Me_2P(CH_2)_2B(iBu)_2$ was measured.) At room temperature, the solid turned liquid. Distillation under high vacuum ($p = 3\times10^{-6}$ bar) at 20 °C yielded **1** (2.01 g, 9.39 mmol, 52%). IR (ATR): $\tilde{\nu}$ = 2944 (m), 2891 (w), 2860 (m), 1461 (w), 1419 (w), 1375 (m), 1347 (vs), 1315 (s), 1289 (m), 1250 (w), 1207 (vw), 1155 (w), 1091 (vw), 1056 (vw), 1034 (vw), 980 (s), 936 (s), 890 (w), 858 (w), 816 (w), 750 (w), 731 (m), 697 (w), 647 (vw), 577 (vw), 500 (vw), 412 cm^{-1} (vw); ^{1}H NMR (300 MHz, C_6D_6): δ = 2.36 (d, ^2J(P,H) = 12.1 Hz, 1H; H_{ylid}), 2.26 (nonet, ^3J(H,H) = 6.7 Hz, 2H; H_{iBuCH}), 2.21 (nonet, ^3J(H,H) = 6.7 Hz, 2H; H_{iBuCH}), 1.28 (d, ^3J(H,H) = 6.8 Hz, 2H; H_{iBuCH2}), 1.27 (d, ^3J(H,H) = 6.5 Hz, 6H; H_{iBuCH3}), 1.16 (d, ^3J(H,H) = 6.5 Hz, 6H; H_{iBuCH3}), 1.12 (d, ^3J(H,H) = 7.2 Hz, 1H; H_{iBuCH2}), 1.12 (d, ^3J(H,H) = 7.2 Hz, 1H; H_{iBuCH2}), 0.86 ppm (d, ^2J(P,H) = 12.6 Hz, 9H; H_{PMe3}); ^{11}B NMR (96 MHz, C_6D_6): δ = 54.7 ppm (s); ^{13}C{^{1}H} NMR (75 MHz, C_6D_6): δ = 48.5 (brs, C_{ylid}), 37.2 (brs, C_{iBuCH2}), 36.0 (brs, C_{iBuCH2}), 27.3 (s, C_{iBuCH1}), 27.3 (s, C_{iBuCH1}), 26.7 (s, C_{iBuCH3}), 26.7 (s, C_{iBuCH2}), 17.6 ppm (d, ^1J(P,C) = 56.2 Hz, C_{PMe3}); ^{31}P{^{1}H} NMR (121 MHz, C_6D_6): δ = 2.03 ppm (s); HRMS (EI): m/z calcd for $C_{12}H_{28}{}^{11}BP$: 214.20216; found: 214.20214; elemental analysis calcd % for $C_{12}H_{28}BP$: P 14.46, B 5.05; found: P 14.40, B 5.08; cryoscopy (benzene, g mol^{-1}): calcd: 214.14; found: 212.0.

Synthesis of 3

A Schlenk tube with a solution of **1** (0.864 g, 1.00 mL, 4.03 mmol) in toluene (10 mL) was degassed with two freeze–pump–thaw cycles and subsequently purged with CO. The reaction mixture was stirred and heated to 70 °C for 3 h. The solution was evaporated to dryness. Pentane (20 mL) was added to the residue, yielding a thin suspension. The suspension was filtered. The filtrate was reduced until crude **3** precipitated. Recrystallisation in boiling pentane, removal of the supernatant layer, and drying under high vacuum, yielded (250 mg, 0.548 mmol, 14%) pure **3** (both diastereomers) as colorless crystals. Suitable crystals for XRD were obtained by solving **3** in a small amount of boiling hexane and cooling the solution very slowly to room temperature. M.p. 181 °C; IR (ATR): $\tilde{\nu}$ = 2936 (m), 1893 (w), 2850 (s), 2802 (w), 1451 (m), 1437 (s), 1356 (vw), 1331 (w), 1311 (w), 1288 (m), 1242 (w), 1159 (w), 1132 (w), 1107 (m), 1077 (m), 970 (s), 944 (vs), 907 (s), 861 (s), 823 (m), 748 (vs), 718 (s), 691(vs),648 (m), 620 (m), 602 (m), 574 (m), 546 (s), 525 (vs), 497 (s), 485 (s), 469 (m), 459 (m), 449 (m), 440 (m), 430 (s), 421 (s), 410 (m), 401 (m), 392 (m), 382 cm^{-1} (m); ^{1}H NMR (signal assignment, if necessary, with ^{1}H{^{11}B}; 300 MHz, C_6D_6): δ = 3.54 (d, ^2J(P,H) = 32.1 Hz, $H_{diastereomer1\_C=C}$, 0.5H), 3.53 (d, ^2J(P,H) = 32.1 Hz, 0.5H; $H_{diastereomer2\_C=C}$), 2.35–2.17 (m, 2H; H_{iBuCH1}), 2.04–1.82 (m, 2H; H_{iBuCH1}), 1.46 (d, ^3J(H,H) = 6.5 Hz, 3H; H_{iBuCH3}), 1.43 (d, ^3J(H,H) = 6.6 Hz, 3H; H_{iBuCH3}), 1.37 (d, ^3J(H,H) = 6.6 Hz, 3H; H_{iBuCH3}), 1.37 (d, ^3J(H,H) = 6.6 Hz, 3H; H_{iBuCH3}), 1.34 (d, ^3J(H,H) = 6.6 Hz, 3H; H_{iBuCH3}), 1.29 (d, ^3J(H,H) = 6.5 Hz, 3H; H_{iBuCH3}), 1.29 (d, ^3J(H,H) = 6.5 Hz, 3H; H_{iBuCH3}), 1.28 (d, ^3J(H,H) = 6.5 Hz, 3H; H_{iBuCH3}), 1.14 (dd, ^2J(H,H) = 14.2 Hz, ^3J(H,H) = 7.5 Hz, 1H; H_{iBuCH2}), 1.08 (dd, ^2J(H,H) = 13.7 Hz, ^3J(H,H) = 5.5 Hz, 1H; H_{iBuCH2}), 1.00 (d, ^2J(P,H) = 12.5 Hz, 9H; H_{BCPMe3}), 0.92 (dd, ^2J(H,H) = 12.5 Hz, ^3J(H,H) = 5.1 Hz, 1H; H_{iBuCH2}), 0.85 (dd, ^2J(H,H) = 12.9 Hz, ^3J(H,H) = 6.1 Hz, 1H; H_{iBuCH2}), 0.89 (d, ^2J(P,H) = 13.5 Hz, 9H; H_{CCPMe3}), 0.63 (dd, ^2J(H,H) = 14.1 Hz, ^3J(H,H) = 3.7 Hz, 1H; H_{iBuCH2}), 0.54 (dd, ^2J(H,H) = 14.2 Hz, ^3J(H,H) = 4.7 Hz, 1H; H_{iBuCH2}), 0.36 (dd, ^2J(H,H) = 12.8 Hz, ^3J(H,H) = 5.0 Hz, 1H; H_{iBuCH2}), 0.32 (d, ^2J(P,H) = 22.8 Hz, 1H; $H_{BC(H)P}$), 0.31 ppm (dd, ^2J(H,H) = 12.2 Hz, ^3J(H,H) = 5.1 Hz, 1H; H_{iBuCH2}); ^{11}B NMR (96 MHz, C_6D_6): δ = 7.2 (brs), −9.4 ppm (s); ^{13}C{^{1}H} NMR (75 MHz, C_6D_6): δ = 231.9 (brs, C_{CO}), 59.3 (d, ^1J(C,P) = 88.2 Hz, C_{PCC}), 40.2 (brs, C_{iBuCH2}), 29.6 (s, C_{iBuCH3}), 29.1 (s, C_{iBuCH3}), 29.0 (s, C_{iBuCH3}), 28.9 (s, C_{iBuCH3}), 28.6 (s, s, C_{iBuCH}), 28.6 (s, C_{iBuCH3}), 27.7 (s, C_{iBuCH3}), 27.0 (s, C_{iBuCH}), 27.0 (s, C_{iBuCH}), 26.9 (s, C_{iBuCH3}), 15.4 (d, ^1J(P,C) = 52.1 Hz, C_{BCPMe}), 14.6 (brs, C_{BCP}) 12.4 ppm (d, ^1J(P,C) = 58.0 Hz, C_{CCPMe}); ^{31}P{^{1}H} NMR (121 MHz, C_6D_6): δ = 22.8 (s,$P_{diastereomer1\_BCP}$), 22.7 (s, $P_{diastereomer2\_BCP}$), −4.23 ppm (s, P_{CCP}); APCI-MS: decomposition; elemental analysis calcd (%) for $C_{25}H_{56}B_2OP_2$: C 65.81, H 12.37; found: C 65.64, H 12.32.

Synthesis of 4

A solution of **1** (700 mg, 3.27 mmol) in toluene (10 mL) was degassed with two freeze–pump–thaw cycles and subsequently purged with 1.1 bar CO_2. The solution was stirred and heated to 90 °C overnight. The solvent and all volatile compounds were evaporated under high vacuum. After removing all volatile compounds, the crude product was only slightly soluble in toluene. Crude product **4** was recrystallized in toluene, yielding, after removal of the supernatant layer and drying under high vacuum, colorless crystalline **4** (538 mg, 0.657 mmol, 60%). Crystals suitable for XRD were obtained by dissolving a small amount of **4** in hot toluene and cooling the solution very slowly to room temperature. M.p. 174 °C (dec); IR (ATR): $\tilde{\nu}$ = 2983 (vw), 2937 (w), 2854 (w), 2792 (vw), 1592 (m), 1579 (m), 1490 (vs), 1452 (vs), 1407 (m), 1373 (vw), 1356 (vw), 1318 (m), 1291 (w), 1245 (m), 1179 (w), 1100 (m), 1058 (w), 982 (s), 964 (s), 947 (s), 898 (w), 865 (w), 840 (m), 816 (w), 789 (m), 756 (m), 729 (vw), 681 (m), 629 (vw), 585 (w), 534 (vw), 506 (vw), 464 (w), 419 (vw), 404 cm^{-1} (vw); ^{1}H NMR (300 MHz, [D$_8$]THF): δ = 2.03 (d, ^2J(P,H) = 15.2 Hz, 12H; H_{PMe3}), 1.80 (d, ^2J(P,H) = 14.1 Hz, 18H; H_{PMe4}), 1.76–1.65 (m, 4H; H_{iBuCH_ring}),1.59 (sept, ^3J(H,H) = 6.5 Hz, 2H; H_{iBuCH_bridge}), 0.86 (d, J = 6.5 Hz, 24H; H_{iBuCH3_ring}), 0.84 (d, J = 6.5 Hz, 12H; H_{iBuCH3_bridge}), 0.66 (d, J = 6.9 Hz, 4H; H_{iBuCH2_bridge}) 0.28 ppm (brs, 8H; H_{iBuCH2_ring}); ^{11}B NMR (96 MHz, [D$_8$]THF): δ = −14.9 ppm (brs); ^{13}C{^{1}H} NMR (101 MHz, [D$_8$]THF): δ = 174.0 (brs, C_{CO2}), 171.8 (brs, C_{CO2}), 57.5 (d, ^1J(P,C) = 128 Hz, C_{PCCO}) 35.2 (brs, C_{iBuCH2_ring}), 32.6 (brs, C_{iBuCH2_bridge}), 27.9 (s, C_{iBuCH3_ring}), 27.0 (s, C_{iBuCH3_bridge}), 27.0 (s, C_{iBuCH_bridge}), 26.5 (s, C_{iBuCH_ring}), 13.9 (d, ^1J(P,C) = 62.0 Hz, C_{PMe3}), 9.9 ppm (d, ^1J(P,C) = 44.8 Hz, C_{PMe4}); ^{31}P{^{1}H} NMR (121 MHz, [D$_8$]THF): δ = 25.7 (s, P_{Me4}), 9.9 ppm (s, P_{ylid}); APCI-MS: decomposition; elemental analysis calcd (%) for $C_{40}H_{84}B_3O_8P_3$: C 58.70, H 10.35; found: C 58.34, H 10.73.

Synthesis of 5

A solution of **1** (500 mg) in hexane (8 mL) and a solution of PhNCO (258 mg, 2.16 mmol) in hexane (8 mL) were combined under stirring at room temperature. Stirring was discontinued and crude product **5** recrystallized. After 1 h reaction time, the supernatant layer was removed and the colorless crystals were dried under high vacuum. The crude product was dissolved in benzene and filtered. Evaporation of the solvent and drying under high vacuum yielded pure **5** (282 mg, 0.846 mg, 39%). Crystals suitable for XRD were obtained by slow solvent evaporation of a solution of **5** in benzene. M.p. 62 °C (dec); IR (ATR): $\tilde{\nu}$ = 2942 (vw), 2859 (vw), 1601 (vw), 1573 (vw), 1542 (vs), 1502 (m), 1449 (vw), 1419 (w), 1402 (w), 1374 (vw), 1359 (vw), 1322 (vw), 1308 (vw), 1292 (w), 1253 (vw), 1241 (w), 1165 (vw), 1108 (w), 1075 (vw), 1027 (m), 972 (s), 948 (s), 896 (vw), 880 (vw), 866 (vw), 819 (vw), 806 (vw), 752 (m), 733 (w), 692 (s), 662 (vw), 598 (vw), 570 (vw), 504 (m), 434 cm^{-1} (vw); ^{1}H NMR (300 MHz, C_6D_6): δ = 7.28–7.26 (m, 4H; $H_{ortho/meta}$), 6.92–6.83 (m, 1H; H_{para}), 2.62 (d, ^2J(P,H) = 18.2 Hz, 1H; H_{ylide}), 2.15 (sept, ^3J(H,H) = 6.6 Hz, 2H; H_{iBuCH}), 1.29 (d, ^3J(H,H) = 6.6 Hz, 12H; H_{iBuCH3}), 1.16 (d, ^3J(H,H) = 6.6 Hz, 4H; H_{iBuCH2}), 0.75 ppm (d, ^2J(P,H) = 13.6 Hz, 9H); ^{11}B NMR (96 MHz, C_6D_6): δ = 16.5 ppm (br s); ^{13}C{^{1}H} NMR (75 MHz, C_6D_6): δ = 171.2 (d, ^2J(P,C) = 4.7 Hz, C_{NCO}), 143.1 (s, C_{ipso}), 129.3 (s, $C_{ortho/meta}$), 120.5 (s, C_{para}), 118.0 (s, $C_{ortho/meta}$), 35.3 (d, ^1J(P,C) = 115.8 Hz, C_{ylid}), 34.1 (br s, C_{iBuCH2}), 27.3 (s, C_{iBuCH3}), 26.3 (s, C_{iBuCH1}), 12.6 ppm (d, ^1J(P,C) = 60,7 Hz, C_{MeP}); ^{31}P{^{1}H} NMR (121 MHz, C_6D_6): δ = 6.2 ppm (s); APCI-MS: decomposition; elemental analysis calcd (%) for $C_{19}H_{33}BNOP$: C 68.48, H 9.98, N 4.20; found: C 68.31, H 9.75, N 4.28.

Synthesis of 6

A solution of **1** (250 mg, 1.16 mmol) in toluene (5 mL) was slowly added to a solution of PhNCS (150 mg, 1.16 mmol) in toluene (5 mL) under vigorous stirring. The solution turned slowly yellow. The solution was stirred at room temperature overnight and subsequently all volatile compounds were removed in vacuo. The orange residue was dissolved in toluene (2 mL) and layered with pentane (15 mL). After diffusion, the solution was filtered off from the resulting precipitate. The precipitate was washed with pentane (3×15 mL). The precipitate was dissolved in toluene (1 mL) and layered with pentane (15 mL). After diffusion, the supernatant layer was removed and the residue was dried in vacuo. This procedure yielded **6** as yellow crystals (73 mg, 0.21 mmol, 18%). M.p. 89 °C (dec); IR (ATR): $\tilde{\nu}$ = 2949 (w), 2911 (vw), 2863 (vw), 1594 (w), 1493 (s), 1405 (m), 1304 (m), 1260 (w), 1163 (s), 1100 (vs), 979 (vs), 905 (m), 757 (m), 740 (w), 695 (vs), 670 (w), 605 (w), 605 (w), 567 (w), 541 (w), 529 (m), 484 (s), 474 (vs), 464 (vs), 456 (vs), 444 (s), 427 (m), 414 (m), 399 (m), 388 (m), 380 cm^{-1} (vw); ^{1}H NMR (400 MHz, C_6D_6): δ = 7.57–7.54 (m, 2H; H_{ortho}), 7.26–7.21 (m, 2H; H_{meta}), 6.92 (tt, ^3J(H,H) = 7.5, 1.1 Hz, 1H; H_{para}), 3.55 (d, 1H, H_{ylid}), 2.37 (nonet, ^3J(H,H) = 6.6 Hz, 1H; $H_{Bu\text{-}CH}$), 2.35 (nonet, ^3J(H,H) = 6.6 Hz, 1H; $H_{Bu\text{-}CH}$), 1.40 (d, ^3J(H,H) = 6.3 Hz, 4H; $H_{Bu\text{-}CH2}$), 1.35 (d, ^3J(H,H) = 6.6 Hz, 12H; $H_{Bu\text{-}CH3}$), 0.78 ppm (d, ^3J(H,H) = 13.4 Hz, 9H; $H_{P\text{-}Me}$); ^{11}B NMR (96 MHz, C_6D_6): δ = 15.1 ppm (s); ^{13}C{^{1}H} NMR (101 MHz, C_6D_6): δ = 175.8 (d, ^2J(P,C) = 13.6 Hz, C_{NCS}), 144.9 (s, C_{ipso}), 129.1 (s, C_{meta}), 122.8 (s, C_{para}), 122.7 (s, C_{ortho}), 49.6 (d, ^1J(P,C) = 122.6 Hz, C_{ylid}), 36.26 (br s, $C_{Bu\text{-}CH2}$), 27.6 (s, C_{iBuCH}), 27.2 (s, C_{iBuCH3}), 12.2 ppm (d, ^1J(P,C) = 60.8 Hz, $C_{P\text{-}Me}$); ^{31}P{^{1}H} NMR (162 MHz, C_6D_6): δ = 5.5 ppm (s); APCI-MS: decomposition; elemental analysis calcd (%) for $C_{19}H_{33}BNPS$: S 9.18, N 4.01, C 65.33, H 9.52; found: S 8.78, N 4.02, C 64.98, H 9.23.

X-ray crystallographic studies

A suitable crystal was covered in mineral oil (Aldrich) and mounted on a glass fiber or a mylar loop. The crystal was transferred directly to the cold stream of a STOE IPDS 2 diffractometer. All structures were solved by using SHELXS/T[27] with Olex2.[28] The remaining non-hydrogen atoms were located from successive difference Fourier map calculations. The refinements were carried out by using full-matrix least-squares techniques on F^2 with the program SHELXL.[29] In each case, the locations of the largest peaks in the final difference Fourier map calculations, as well as the magnitude of the residual electron densities, were of no chemical significance. Details on the data refinement are provided in the Supporting Information.

CCDC-1920465, 1920466, 1920467, and 1920468 contain the supplementary crystallographic data for this paper. These data are provided free of charge by The Cambridge Crystallographic Data Centre.

Crystal data for 3

$C_{25}H_{56}B_2OP_2$, M_r = 456.25, monoclinic, $P2_1/c$ (no. 14), a = 16.2691(8) Å, b = 10.2295(8) Å, c = 18.3578(10) Å, β = 92.996(4)°, α = γ = 90°, V = 3051.0(3) Å^3, T = 200 K, Z = 4, Z' = 1, μ($Mo_{K\alpha}$) = 0.156, 17638 reflections measured, 17638 unique (R_{int} = 0.0237), which were used in all calculations. The final wR_2 was 0.1390 (all data) and R_1 was 0.0630 ($I > 2(I)$).

Crystal data for 4

$C_{47}H_{92}B_3O_8P_3$, M_r = 910.54, triclinic, $P\bar{1}$ (no. 2), a = 10.3051(3) Å, b = 15.3631(5) Å, c = 18.5740(7) Å, α = 82.113(3)°, β = 82.493(3)°, γ = 79.034(3)°, V = 2843.0(2) Å^3, T = 200(2) K, Z = 2, Z' = 1, μ($Mo_{K\alpha}$) = 0.148, 28135 reflections measured, 15190 unique (R_{int} = 0.0273), which were used in all calculations. The final wR_2 was 0.1634 (all data) and R_1 was 0.0523 ($I > 2(I)$).

Crystal data for 5

$C_{19}H_{33}BNOP$, M_r = 333.24, monoclinic, $P2_1/n$ (no. 14), a = 11.900(2) Å, b = 13.558(3) Å, c = 12.590(3) Å, β = 95.70(3)°, α = γ = 90°, V = 2021.2(7) Å^3, T = 200 K, Z = 4, Z' = 1, μ($Mo_{K\alpha}$) = 0.140, 14929 reflections measured, 5455 unique (R_{int} = 0.0579), which were used in all calculations. The final wR_2 was 0.1109 (all data) and R_1 was 0.0467 ($I > 2(I)$).

Crystal data for 6

$C_{19}H_{33}BNPS$, M_r = 349.30, triclinic, $P\bar{1}$ (no. 2), a = 9.5890(19) Å, b = 10.106(2) Å, c = 11.551(2) Å, α = 86.62(3)°, β = 79.45(3)°, γ = 71.20(3)°, V = 1041.7(4) Å^3, T = 200 K, Z = 2, Z' = 1, μ($Mo_{K\alpha}$) = 0.232, 11612 reflections measured, 5572 unique (R_{int} = 0.0360), which were used in all calculations. The final wR_2 was 0.1460 (all data) and R_1 was 0.0429 ($I > 2(I)$).

Acknowledgements

We gratefully acknowledge Dr. Christopher E. Anson and Hanna E. Wagner for their help with the crystal structures. We also gratefully acknowledge Wolfram Feuerstein for carefully reading the manuscript.

Conflict of interest

The authors declare no conflict of interest.

Keywords: boranes · phosphorus · quantum chemistry · small ring systems · ylides

[1] G. H. Spikes, J. C. Fettinger, P. P. Power, *J. Am. Chem. Soc.* **2005**, *127*, 12232 – 12233.

[2] G. C. Welch, R. R. S. Juan, J. D. Masuda, D. W. Stephan, *Science* **2006**, *314*, 1124.

[3] a) R. L. Melen, *Science* **2019**, *363*, 479; b) M.-A. Légaré, C. Pranckevicius, H. Braunschweig, *Chem. Rev.* **2019**, *119*, 8231 – 8261; c) T. Chu, G. I. Nikonov, *Chem. Rev.* **2018**, *118*, 3608 – 3680; d) M.-A. Légaré, G. Bélanger-Chabot, R. D. Dewhurst, E. Welz, I. Krummenacher, B. Engels, H. Braunschweig, *Science* **2018**, *359*, 896; e) S. Dagorne, R. Wehmschulte, *ChemCatChem* **2018**, *10*, 2509 – 2520; f) M.-A. Légaré, M.-A. Courtemanche, É. Rochette, F.-G. Fontaine, *Science* **2015**, *349*, 513; g) T. J. Hadlington, M. Driess, C. Jones, *Chem. Soc. Rev.* **2018**, *47*, 4176 – 4197; h) A. Merk, H. Großekappenberg, M. Schmidtmann, M.-P. Luecke, C. Lorent, M. Driess, M. Oestreich, H. F. T. Klare, T. Müller, *Angew. Chem. Int. Ed.* **2018**, *57*, 15267 – 15271; *Angew. Chem.* **2018**, *130*, 15487 – 15492; i) P. P. Power, *Acc. Chem. Res.* **2011**, *44*, 627 – 637; j) P. P. Power, *Nature* **2010**, *463*, 171; k) S. Wang, T. J. Sherbow, L. A. Berben, P. P. Power, *J. Am. Chem. Soc.* **2018**, *140*, 590 – 593; l) C. Weetman, S. Inoue, *ChemCatChem* **2018**, *10*, 4213 – 4228.

[4] a) D. W. Stephan, *Science* **2016**, *354*, aaf7229; b) D. W. Stephan, G. Erker, *Angew. Chem. Int. Ed.* **2010**, *49*, 46 – 76; *Angew. Chem.* **2010**, *122*, 50 – 81; c) D. W. Stephan, *Acc. Chem. Res.* **2015**, *48*, 306 – 316; d) D. W. Stephan, *Dalton Trans.* **2009**, 3129 – 3136; e) D. W. Stephan, G. Erker, *Angew. Chem. Int. Ed.* **2015**, *54*, 6400 – 6441; *Angew. Chem.* **2015**, *127*, 6498 – 6541; f) J. Paradies, *Coord. Chem. Rev.* **2019**, *380*, 170 – 183.

[5] a) M. Melaimi, R. Jazzar, M. Soleilhavoup, G. Bertrand, *Angew. Chem. Int. Ed.* **2017**, *56*, 10046 – 10068; *Angew. Chem.* **2017**, *129*, 10180 – 10203; b) G. D. Frey, V. Lavallo, B. Donnadieu, W. W. Schoeller, G. Bertrand, *Science* **2007**, *316*, 439.

[6] a) J. Escudié, C. Couret, H. Ranaivonjatovo, *Coord. Chem. Rev.* **1998**, *178*, 565 – 592; b) R. C. Fischer, P. P. Power, *Chem. Rev.* **2010**, *110*, 3877 – 3923; c) V. Y. Lee, A. Sekiguchi, *Organometallics* **2004**, *23*, 2822 – 2834; d) H. Ottosson, P. G. Steel, *Chem. Eur. J.* **2006**, *12*, 1576 – 1585; e) K. K. Milnes, L. C. Pavelka, K. M. Baines, *Chem. Soc. Rev.* **2016**, *45*, 1019 – 1035; f) J. W. Taylor, A. McSkimming, C. F. Guzman, W. H. Harman, *J. Am. Chem. Soc.* **2017**, *139*, 11032 – 11035; g) A.-F. Pécharman, A. L. Colebatch, M. S. Hill, C. L. McMullin, M. F. Mahon, C. Weetman, *Nat. Commun.* **2017**, *8*, 15022; h) S. J. Geier, T. M. Gilbert, D. W. Stephan, *J. Am. Chem. Soc.* **2008**, *130*, 12632 – 12633; i) Z. Dong, L. Albers, M. Schmidtmann, T. Müller, *Chem. Eur. J.* **2019**, *25*, 1098 – 1105.

[7] a) Y. Su, Y. Li, R. Ganguly, R. Kinjo, *Angew. Chem. Int. Ed.* **2018**, *57*, 7846 – 7849; *Angew. Chem.* **2018**, *130*, 7972 – 7975; b) B. Wang, Y. Li, R. Ganguly, H. Hirao, R. Kinjo, *Nat. Commun.* **2016**, *7*, 11871.

[8] a) T. Tomioka, Y. Takahashi, T. Maejima, *Org. Biomol. Chem.* **2012**, *10*, 5113 – 5118; b) T. Tomioka, R. Sankranti, T. G. Vaughan, T. Maejima, T. Yanase, *J. Org. Chem.* **2011**, *76*, 8053 – 8058.

[9] a) H. J. Bestmann, T. Arenz, *Angew. Chem.* **1984**, *96*, 363 – 364; b) O. I. Kolodiazhnyi, *Tetrahedron* **1996**, *52*, 1855 – 1929; c) for nice recent developments in ylide chemistry, see for example: L. T. Scharf, D. M. Andrada, G. Frenking, V. H. Gessner, *Chem. Eur. J.* **2017**, *23*, 4422 – 4434; d) T. Scherpf, K.-S. Feichtner, V. H. Gessner, *Angew. Chem. Int. Ed.* **2017**, *56*, 3275 – 3279; *Angew. Chem.* **2017**, *129*, 3323 – 3327; e) C. Schwarz, T. Scherpf, I. Rodstein, J. Weismann, K.-S. Feichtner, V. H. Gessner, *ChemistryOpen* **2019**, *8*, 621 – 626.

[10] a) M. Radius, F. Breher, *Chem. Eur. J.* **2018**, *24*, 15744 – 15749; b) for a closely related paper of our group see: S. Styra, M. Radius, E. Moos, A. Bihlmeier, F. Breher, *Chem. Eur. J.* **2016**, *22*, 9508 – 9512.

[11] H. J. Bestmann, *Chem. Ber.* **1962**, *95*, 58 – 63.

[12] a) H. Schmidbaur, *Acc. Chem. Res.* **1975**, *8*, 62 – 70; b) H. Schmidbaur, U. Deschler, B. Milewski-Mahrla, B. Zimmer-Gasser, *Chem. Ber.* **1981**, *114*, 608 – 619; c) H.-J. Cristau, A. Perraud, E. Manginot, E. Torreilles, *Phosphorus Sulfur Silicon Relat. Elem.* **1993**, *75*, 7 – 10; d) H.-J. Cristau, *Chem. Rev.* **1994**, *94*, 1299 – 1313; e) H.-J. Cristau, Y. Ribeill, F. Plenat, L. Chiche, *Phosphorus Sulfur Silicon Relat. Elem.* **1987**, *30*, 135 – 138.

[13] Y. Canac, C. Lepetit, M. Abdalilah, C. Duhayon, R. Chauvin, *J. Am. Chem. Soc.* **2008**, *130*, 8406 – 8413.

[14] H. Böhrer, N. Trapp, D. Himmel, M. Schleep, I. Krossing, *Dalton Trans.* **2015**, *44*, 7489 – 7499.

[15] N. Inamoto, S. Masuda, *Chem. Lett.* **1982**, *11*, 1003 – 1006.

[16] J. Berkowitz, G. B. Ellison, D. Gutman, *J. Phys. Chem.* **1994**, *98*, 2744 – 2765.

[17] H. Nöth, B. Wrackmeyer, *Chem. Ber.* **1981**, *114*, 1150 – 1156.

[18] a) B. M. Mikhailov, Y. N. Bubnov, *Zh. Obshch. Khim.* **1961**, *31*, 577 – 582; b) E. Rothgery, R. Köster, *Liebigs Ann.* **1974**, 101 – 111.

[19] N. W. Mitzel, D. H. Brown, S. Parsons, P. T. Brain, C. R. Pulham, D. W. H. Rankin, *Angew. Chem. Int. Ed.* **1998**, *37*, 1670 – 1672; *Angew. Chem.* **1998**, *110*, 1767 – 1770.

[20] a) M. Schlosser, T. Jenny, B. Schaub, *Heteroat. Chem.* **1990**, *1*, 151 – 156; b) S. M. Bachrach, *J. Org. Chem.* **1992**, *57*, 4367 – 4373.

[21] One referee of this paper suggested that splitting in the NMR signals of **3** could also be due to *cis–trans* isomerism/bond rotation of the C–C bond of the P–C=C subunit. We thank the reviewer very much for this helpful hint. Although such isomerism is also possible, we believe that steric repulsion of the Me_3P and *i*Bu substituents would most likely not lead to the 1:1 intensities of the signals. We also noted that T-dependent NMR spectroscopy measurements at higher temperatures did not alter the 1:1 integration of the signals (see Figures S28 and S29 in the Supporting Information).

[22] G. Margraf, H.-W. Lerner, M. Bolte, *Acta Crystallogr. Sect. E* **2002**, *58*, o546 – o547.

[23] C. Chauvier, P. Thuéry, T. Cantat, *Chem. Sci.* **2016**, *7*, 5680 – 5685.

[24] R. Köster, D. Simić, M. A. Grassberger, *Liebigs Ann.* **1970**, *739*, 211 – 219.

[25] U. Höbel, H. Nöth, H. Prigge, *Chem. Ber.* **1986**, *119*, 325 – 337.

[26] J. Meiners, A. Friedrich, E. Herdtweck, S. Schneider, *Organometallics* **2009**, *28*, 6331 – 6338.

[27] a) G. M. Sheldrick, *Crystallographic Computing 3*, **1985**; b) G. Sheldrick, *Acta Crystallogr. Sect. A* **2015**, *71*, 3 – 8.

[28] O. V. Dolomanov, L. J. Bourhis, R. J. Gildea, J. A. K. Howard, H. Puschmann, *J. Appl. Crystallogr.* **2009**, *42*, 339 – 341.

[29] G. Sheldrick, *Acta Crystallogr. Sect. C* **2015**, *71*, 3 – 8.

Manuscript received: June 11, 2019
Revised manuscript received: July 19, 2019
Accepted manuscript online: July 29, 2019
Version of record online: August 23, 2019

